Bioorganic & Medicinal Chemistry 18 (2010) 7475–7485

Contents lists available at ScienceDirect

Bioorganic & Medicinal Chemistry

journal homepage: www.elsevier.com/locate/bmc

2-Hexadecynoic acid inhibits plasmodial FAS-II enzymes and arrests erythrocytic and liver stage *Plasmodium* infections

Deniz Tasdemir [a,*], David Sanabria [b], Ina L. Lauinger [a], Alice Tarun [c,d], Rob Herman [c], Remo Perozzo [e], Mire Zloh [a], Stefan H. Kappe [c], Reto Brun [f], Néstor M. Carballeira [b,*]

[a] Department of Pharmaceutical and Biological Chemistry, School of Pharmacy, University of London, 29-39 Brunswick Square, London WC1N 1AX, United Kingdom
[b] Department of Chemistry, University of Puerto Rico, PO Box 70377, San Juan, PR 00936-8377, USA
[c] Seattle Biomedical Research Institute, 307 Westlake Avenue N, Suite 500, Seattle, WA 98109-5219, USA
[d] Department of Infectious Diseases and Microbiology, University of Pittsburgh, 130 Desoto St, Pittsburgh, PA 15261, USA
[e] School of Pharmaceutical Sciences, University of Geneva, Quai Ernest-Ansermet 30, 1211 Geneva 4, Switzerland
[f] Department of Medical Parasitology and Infection Biology, Swiss Tropical Institute, Socinstr. 57, Basel 4002, Switzerland

ARTICLE INFO

Article history:
Received 2 June 2010
Revised 14 July 2010
Accepted 29 August 2010
Available online 18 September 2010

Keywords:
Hexadecynoic acid
Malaria
Liver stage
Blood stage
Protozoa
Type II fatty acid biosynthesis

ABSTRACT

Acetylenic fatty acids are known to display several biological activities, but their antimalarial activity has remained unexplored. In this study, we synthesized the 2-, 5-, 6-, and 9-hexadecynoic acids (HDAs) and evaluated their in vitro activity against erythrocytic (blood) stages of *Plasmodium falciparum* and liver stages of *Plasmodium yoelii* infections. Since the type II fatty acid biosynthesis pathway (*Pf*FAS-II) has recently been shown to be indispensable for liver stage malaria parasites, the inhibitory potential of the HDAs against multiple *P. falciparum* FAS-II (*Pf*FAS-II) elongation enzymes was also evaluated. The highest antiplasmodial activity against blood stages of *P. falciparum* was displayed by 5-HDA (IC_{50} value 6.6 μg/ml), whereas the 2-HDA was the only acid arresting the growth of liver stage *P. yoelii* infection, in both flow cytometric assay (IC_{50} value 2-HDA 15.3 μg/ml, control drug atovaquone 2.5 ng/ml) and immunofluorescence analysis (IC_{50} 2-HDA 4.88 μg/ml, control drug atovaquone 0.37 ng/ml). 2-HDA showed the best inhibitory activity against the *Pf*FAS-II enzymes *Pf*FabI and *Pf*FabZ with IC_{50} values of 0.38 and 0.58 μg/ml (IC_{50} control drugs 14 and 30 ng/ml), respectively. Enzyme kinetics and molecular modeling studies revealed valuable insights into the binding mechanism of 2-HDA on the target enzymes. All HDAs showed in vitro activity against *Trypanosoma brucei rhodesiense* (IC_{50} values 3.7–31.7 μg/ml), *Trypanosoma cruzi* (only 2-HDA, IC_{50} 20.2 μg/ml), and *Leishmania donovani* (IC_{50} values 4.1–13.4 μg/ml) with generally low or no significant toxicity on mammalian cells. This is the first study to indicate therapeutic potential of HDAs against various parasitic protozoa. It also points out that the malarial liver stage growth inhibitory effect of the 2-HDA may be promoted via *Pf*FAS-II enzymes. The lack of cytotoxicity, lipophilic nature, and calculated pharmacokinetic properties suggests that 2-HDA could be a useful compound to study the interaction of fatty acids with these key *P. falciparum* enzymes.

1. Introduction

Malaria continues to be a cause of concern in underdeveloped areas of the world. The World Health Organization (WHO) reports around 300 million new cases, and over one million deaths due to malaria each year.[1] Malaria parasite *Plasmodium* has a complex life cycle involving two hosts. The infection is initiated when *Plasmodium* sporozoites enter the human (host 1) through the bite of an infected *Anopheles* mosquito (host 2). The sporozoites inoculated under the skin of the host migrate to the liver, where they infect hepatocytes and begin to develop into merozoites. This so-called liver stage (LS) or exoerythrocytic forms takes 2–16 days, depending on the *Plasmodium* species, then thousands of LS merozoites are released into the bloodstream, where they invade red blood cells and start multiple rounds of the asexual blood stages (BS). The entire asexual BS cycle is completed within 1–2 days, again depending on the *Plasmodium* species, producing large numbers of infected erythrocytes ($>10^{12}$ per host).[2] During the BS, some merozoites transform into the sexual stages, the male and female gametocytes, which can be taken up by mosquitoes during blood meals. Gametocytes undergo fertilization in the mosquito midgut, producing oocyst sporozoites that migrate to the salivary glands, ready to initiate a new round of infection.

Past and current malaria drug discovery has been primarily directed against the easy-to-grow asexual BS, which is responsible

* Corresponding authors. Tel.: +44 20 77535845; fax: +44 20 77535909 (D.T.); tel.: +1 787 764 0000x4791; fax: +1 787 756 8242 (N.M.C.).
E-mail addresses: deniz.tasdemir@pharmacy.ac.uk (D. Tasdemir), nmcarballeira@uprrp.edu (N.M. Carballeira).

0968-0896/$ - see front matter © 2010 Elsevier Ltd. All rights reserved.
doi:10.1016/j.bmc.2010.08.055

for the clinical symptoms as well as mortality and morbidity of the disease. Mainly due to technical challenges and high costs, LS has been little exploited, despite its longer life span (6–7 days in *Plasmodium falciparum*) than the BS (2 days in *P. falciparum*) and the generation of much smaller number of parasites. Recently, a serious consideration has been given to asymptomatic LS parasites as its full inhibition provides true causal malaria prophylaxis, that is, prevents the blood stage infection and its clinical manifestations. The development of molecules inhibiting the growth of *Plasmodium* hepatic forms could be useful in malaria prevention for people living in malaria endemic areas, as well as for refugees and travelers who are exposed to malaria risk for a limited time. Inhibition of LS also reduces the risk of transmission because the generation of the gametocytes will be interrupted.[3] Furthermore, the low parasitic load with limited multiplication substantially reduces the likelihood for drug-resistant forms to emerge. Hepatic stage parasites represent further complication for *Plasmodium vivax* and *Plasmodiun ovale* infections, as some of the parasites in the hepatocytes transform into hypnozoites, which can stay dormant up to several years and cause relapse.[4] A few drugs, for example, atovaquone, 8-aminoquinolines primaquine and tafenoquine are effective against LS, but the primaquine is the only FDA licensed drug. However, its use is restricted, particularly in Africa because of the frequency of genetic glucose-6-phosphate 1-dehydrogenase (G6PD) deficiency. Primaquine is also toxic and has a very short half-life.[4] Many other non-8-aminoquinolines lack oral bioavailability, and a few natural products with anti-LS activity have low selectivity.[5,6] Hence, the search for new natural or synthetic drugs targeting the LS of the malaria parasite is timely and necessary.

Due to inherent technical difficulties in studying the LS *Plasmodium* parasites, little progress has been made in the identification of new LS biological targets for drug discovery and design. Very recent studies[7,8] indicate that LS malaria parasites exhibit an absolute requirement for de novo type II fatty acid biosynthesis (FAS-II), which was previously thought to operate in blood stage.[9] The FAS-II pathway appears to be essential only for late hepatic stages and deletion of critical elongation enzymes such as FabB/F (β-ketoacyl-ACP synthase) and FabZ (β-hydroxyacyl-ACP dehydratase) in *Plasmodium yoelii* cause a failure to generate exoerythrocytic merozoites, that is, inability to cause a BS infection.[7] Similarly, FabI (enoyl-ACP reductase)-deficient *Plasmodium berghei* sporozoites were much less infective in mice and failed to complete liver stage development.[8] These data render the plasmodial FAS-II pathway an attractive target for malaria prophylaxis.

Fatty acids have shown antimalarial activity[10–12] but the literature reports have been scarce and there is not a consensus as to what structural characteristics (i.e., unsaturation level, position or chain length) favor the best antimalarial fatty acids. We believed that a systematic study of the antimalarial activity of a series of isomeric C_{16} acetylenic fatty acids could shed light on the structural properties required for antimalarial activity, in particular how the antimalarial activity depends on the position of the triple bond in a C_{16} acyl chain. For this purpose, we chose an isomeric series of hexadecynoic acids (HDA), that is, the 2-, 5-, 6-, and 9-HDAs, some of which were shown to be antibacterial, antifungal, and antimycobacterial,[13–16] but never investigated for antimalarial potential, and synthesized them. Another reason for choosing C16 acetylenic acids, and not longer or shorter fatty acids (FAs), was because earlier studies indicated that 2-HDA inhibited fatty acid elongation.[17,18] The 2-HDA has recently been shown to inhibit InhA, the enoyl-ACP reductase (FabI) analogue enzyme found in the FAS-II pathway of the tubercle bacillus, *Mycobacterium tuberculosis*.[16] In a recent publication, we reported unsaturated fatty acids inhibiting enoyl-ACP reductases of *P. falciparum* (*Pf*) and *M. tuberculosis*.[19] These facts suggested that C-16 alkynoic acids, especially 2-HDA could target the *Pf*FabI (and potentially other elongation enzymes from *Pf*FAS-II system) and lead to death of LS malaria parasites. Herein we report (a) the synthesis of four HDAs, (b) their in vitro growth inhibitory potential against BS and LS malaria parasites, (c) inhibitory activity against multiple *Pf*FAS-II elongation enzymes, *Pf*FabI, *Pf*FabZ, and *Pf*FabG (β-ketoacyl-ACP reductase), (d) the enzyme kinetics, docking studies, and calculated pharmacokinetic properties, (e) in vitro activity against other parasitic protozoa, that is, *Trypanosoma brucei rhodesiense*, *Trypanosoma cruzi*, and *Leishmania donovani* and (f) Selective toxicity toward primary mammalian and hepatoma cells. Palmitic acid (PA), the parent compound lacking the triple bond was also tested in each assay for comparison.

2. Results

2.1. Synthesis of hexadecynoic acid derivatives

We developed a short and versatile procedure to prepare the 5-, 6-, and 9-hexadecynoic acids as outlined in Figure 1. In general, the appropriate bromo alcohol was protected with *tert*-butyldimethylsilyl chloride (TBSCl) yielding the TBS-protected bromo alcohols in 80–99% yields. Alkyne coupling with the required chain length of the 1-alkynes in the presence of *n*-BuLi in tetrahydrofuran–hexamethylphosphoramide (THF-HMPA) produced the desired TBS-protected alkynols in 23–32% yields. Deprotection of the TBS group with tetrabutylammonium fluoride (TBAF) in THF followed by oxidation of the resulting alcohols with pyridinium chloride (PDC) in dimethylformamide (DMF) afforded the desired hexadecynoic acids in 40–70% yields. The synthesis of the 2-HDA followed an already published procedure[18] wherein commercially available 1-pentadecyne reacted with *n*-BuLi in THF followed by quenching with CO_2 and final protonation with NH_4Cl (Fig. 1). The purity of the synthesized compounds was determined to be >95% by capillary GC–MS and ^{13}C NMR. The spectral data of the synthesized HDAs (Sections 5.2 and 5.3) were in agreement with those published.[13,20,21]

2.2. In vitro antimalarial activity toward *P. falciparum* blood stages

The in vitro antiplasmodial activity of the HDAs against multidrug-resistant *P. falciparum* K1 strain was determined by using the established ^3H-hypoxanthine method. As shown in Table 1, 5-HDA showed the highest antiplasmodial activity among the alkynoic acids with an IC_{50} value of 6.6 μg/ml, followed by the equipotent 2-HDA and 9-HDAs (IC_{50}s 10.4 and 10.3 μg/ml, respectively) and finally 6-HDA (IC_{50} 22.5 μg/ml). Interestingly, the parent compound PA was more active (IC_{50} 3.8 μg/ml) than all acetylenic fatty acids, indicating that a triple bond is not favored for antimalarial activity toward blood stage parasites.

2.3. In vitro activity toward *P. yoelii* liver stages

Next, we wanted to assess life stage selectivity of the HDAs and investigated their growth inhibitory activity against LS malaria parasites. Hepatic stage *P. falciparum* infection in humans is experimentally intractable for practical purposes, hence has remained poorly understood. In contrast, the LS of the disease in the rodent malaria model is amenable to direct experimental interrogation.[2] Thus, we have employed a medium throughput LS growth inhibition assay using rodent *P. yoelii* parasites, which have conserved metabolic and antigenic profile as *P. falciparum*,[22] to infect HepG2:CD81 cell line. Infection was assayed by both flow cytometric (FC) and immunofluorescence analysis (IFA) methods, using atovaquone as reference (Table 1). In the FC assay, the

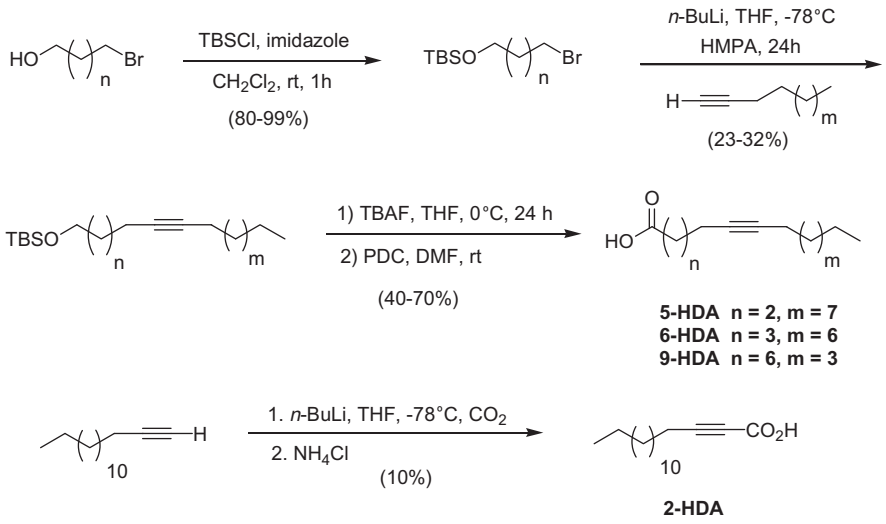

Figure 1. Synthesis of the hexadecynoic acids.

Table 1
Inhibitory activities of the HDAs and palmitic acid (PA) against *P. falciparum* blood stage (BS) and *P. yoelii* liver stage (LS) parasites and *Pf*FAS-II enzymes (FC, flow cytometry; IFA, immunofluorescence analysis)

Compound	*P. falciparum BS*	*P. yoelii LS FC*	*P. yoelii LS IFA*	*Pf*FabI	*Pf*FabZ	*PfFabG*
Standard	0.056[a]	0.0025[b]	0.00037[b]	0.014[c]	0.03[d]	0.32[d]
2-HDA	10.4	15.3	4.88	0.38 ± 0.03	0.58 ± 0.11	3.50 ± 0.35
5-HDA	6.6	>25	>25	3.1 ± 0.57	14.0 ± 1.41	>100
6-HDA	22.5	>25	>25	3.6 ± 0.14	12.0 ± 2.83	>100
9-HDA	10.3	>25	>25	2.8 ± 1.13	12.5 ± 2.12	>100
PA	3.8	>25	>25	>100	>100	>100

IC_{50} values are in μg/ml and represent the average of at least two independent assays performed in duplicates. Reference compounds [a] chloroquine; [b] atovaquone; [c] triclosan; [d] (−)-epigallocatechin gallate.

HepG2:CD81 cells are infected with transgenic *P. yoelii* sporozoites that express green fluorescent protein (*Py*GFP), exposed to compound, and allowed to develop for 43 h to measure infection rates. To verify the results of the FC-based assay and to determine the effects of the drugs on the morphology and development of the LS parasites, IFAs of *P. yoelii*-infected HepG2:CD81 cells were done after drug treatment. In this assay, the LS parasites were detected using a mouse monoclonal antibody against *P. berghei* HSP70 that cross-reacts with *P. yoelii* HSP70[23] and polyclonal antibody against the *P. yoelii* UIS4 protein.[24] The results of both FC and IFA assays are shown in Table 1. In the FC assay, only 2-HDA appeared to be active with an IC_{50} value of 15.3 μg/ml. Atovaquone, a potent inhibitor of LS development, had an IC_{50} value of 2.5 ng/ml. In the IFA, atovaquone was observed to potently inhibit LS development resulting in much smaller parasites with an IC_{50} value of 0.37 ng/ml (Table 1), similar to what has been described before.[25] Smaller LS parasites compared to the control were observed in the IFA after incubation with 2-HDA with an IC_{50} value of 4.88 μg/ml, whereas other alkynoic and palmitic acids had no effect, even at the highest test concentrations. Figure 2 (20× objective magnification) shows an IFA of the late liver stage-infected HepG2:CD81 cells (43 h post-infection) treated with DMSO, PA, and HDAs. The DAPI staining of infected cells (Fig. 2) indicated none of the HDAs to exert toxicity toward the liver cells. Figure 3 displays the close-up fluorescence microscopy images (100× objective magnification) of *P. yoelii* liver stage schizonts detected by antibody against HSP70 protein at 43 h post-infection treated with different concentrations of 2-HDA, as well as DMSO and atovaquone. 2-HDA was non-toxic against hepatoma cells in FC or IFA (see Section 5.6) or against primary mammalian cells (see Sections 2.6. and 5.12) indicating its selective toxicity against the LS parasites.

2.4. *Pf*FAS-II enzyme inhibition studies

In an attempt to understand the mechanism of action of the HDAs against LS parasites, we determined their inhibitory effect against three key enzymes of the fatty acid biosynthesis of *P. falciparum*, that is, *Pf*FabI, *Pf*FabZ, and *Pf*FabG, all of which were recombinantly prepared and assayed following an established procedure.[26] Essentially, the HDAs were inhibitory toward the studied *Pf*Fab enzymes following the order *Pf*FabI > *Pf*FabZ > *Pf*FabG (Table 1). From the data obtained, it became clear that among the studied HDAs, the 2-HDA displayed the best overall inhibitory activity against *Pf*FabI (IC_{50} 0.38 ± 0.03 μg/ml) and *Pf*FabZ (IC_{50} 0.58 ± 0.11 μg/ml), and it was the only inhibitory acetylenic acid against *Pf*FabG (IC_{50} 3.5 ± 0.35 μg/ml). The 5-, 6-, and 9-HDAs were not inhibitory toward *Pf*FabG (IC_{50} >100 μg/ml), and their inhibitory potential against two other target enzymes were 10-fold (*Pf*FabI) to 50-fold (*Pf*FabZ) less. Notably, the parent compound PA was inactive against all enzymes tested even at the highest concentrations (IC_{50} >100 μg/ml). These data indicate that the hepatic stage growth inhibitory activity of 2-HDA may be due to the inhibition of the *Pf*FAS-II enzymes.

2.5. Enzyme kinetics, docking studies, and pharmacokinetic calculations

In order to shed more light into the inhibitory mechanism of 2-HDA, in vitro enzyme kinetic studies as well as molecular modeling (docking) studies were performed. Kinetic studies indicated that 2-HDA inhibits the *Pf*FabI enzyme in a non-competitive manner with respect to crotonyl-CoA and the cofactor NADH (Fig. 4). This implies that 2-HDA binds to the *Pf*FabI enzyme at a site distinct of

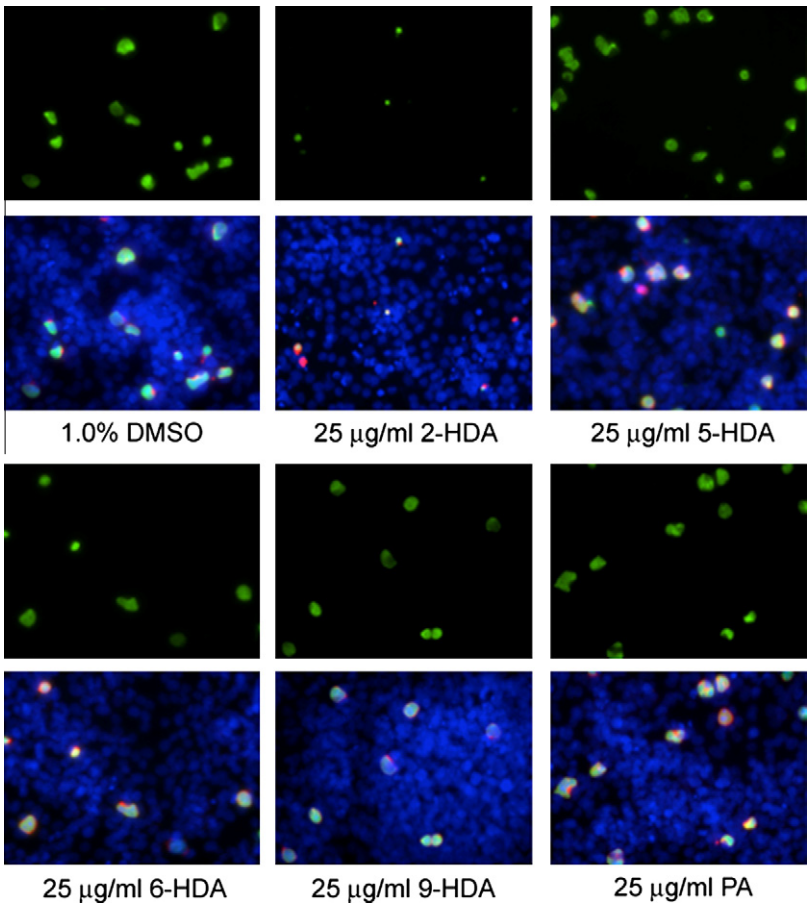

Figure 2. Immunofluorescence microscopy images of *P. yoelii*-infected HepG2:CD81cells at 43 h post-infection treated with 1% DMSO or various compounds taken at 20× objective magnification. The top images for each set of pictures show the liver stage parasites detected by antibody against HSP70 protein (FITC, green) while the bottom images show the merged images of the same section stained with the nuclear stain DAPI (blue) and the liver stage parasites that were doubly stained with antibodies against HSP70 (FITC, green) and UIS4 protein (Texas Red).

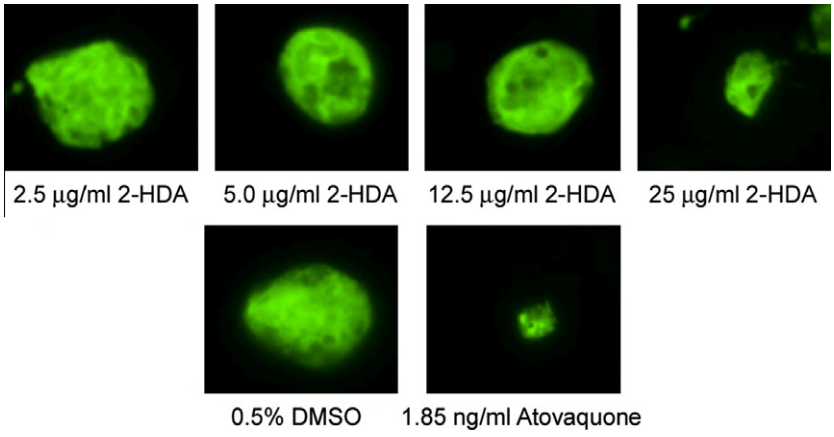

Figure 3. Detailed fluorescence microscopy images of *P. yoelii* liver stage schizonts detected by antibody against HSP70 protein at 43 h post-infection treated with different concentrations of 2-HDA, as well as DMSO and atovaquone (100× objective magnification).

the substrate or the cofactor site. The calculated K_i values are 0.73 μg/ml (=2.90 μM, substrate varied) and 0.65 μg/ml (=2.58 μM, cofactor varied). The inhibition type against the *Pf*FabZ, a dehydratase, which does not require a cofactor, is competitive (K_i 1.2 μg/ml = 4.8 μM) with respect to the substrate (Fig. 5). As shown in Figure 6, 2-HDA inhibits the *Pf*FabG enzyme in a competitive manner when the substrate acetoacetyl-CoA is varied (K_i 3.6 μg/ml = 14.3 μM) and in a non-competitive manner when the cofactor NADPH is varied (K_i 1.5 μg/ml = 6 μM).

Molecular modeling studies supported the predicted binding mode of the acetylenic acids determined by the kinetic studies and revealed insights for understanding the superior enzyme inhibitory activity of 2-HDA over the other HDAs. The molecular docking of these ligands into the binding site of FabZ[27,28] was

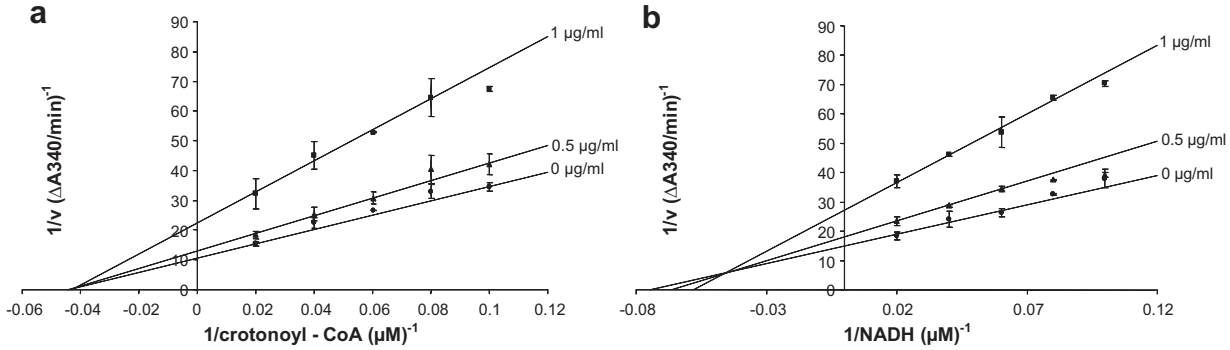

Figure 4. Kinetic plots of the binding of 2-HDA to *Pf*FabI showing a non-competitive inhibition type when the substrate crotonyl-CoA (a) and the cofactor NADH (b) was varied.

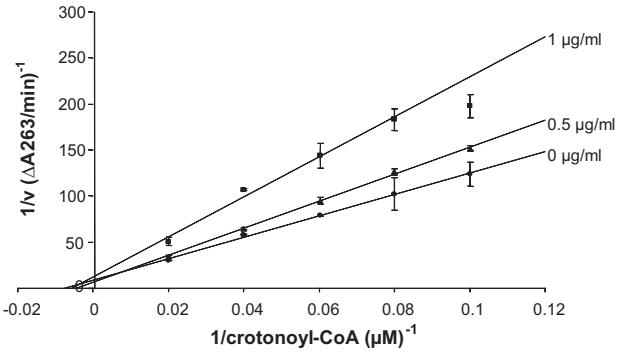

Figure 5. Kinetic plots of the binding of 2-HDA to *Pf*FabZ showing a competitive inhibition type with respect to the substrate crotonyl-CoA.

carried out using the crystal structure given in pdb entry 1z6b. The best fit of ligands and their binding energies predicted by Autodock indicate that all 4 ligands interact favorably with the protein, however the 2-HDA binds most strongly (Fig. 7a). Although there is no direct correlation between activity and binding energy, a trend was observed for energy of interaction ($E_{2\text{-HDA}} < E_{9\text{-HAD}} < E_{5\text{-HDA}} < E_{6\text{-HDA}}$), which corresponds to the trend of activity. Docking studies indicate that only 2-HDA form a hydrogen bond with the backbone NH atoms of Gly142 and Val143 and the electron density of the triple bond of 2-HDA interacts with the active site residue Glu147. These differences most likely explain why the 2-HDA is the most active molecule against *Pf*FabZ.

The docking of ligands into *Pf*FabG site has indicated that all ligands bind closely to the cofactor site, and again the 2-HDA binds with most favorable energy of interactions. The orientation of ligands are different too (results not shown), but further studies would be needed to understand the reasons for such significant difference between activities of 2-HDA and other ligands. The interaction of ligands and the X-ray structure of *Pf*FabI complexed with the NADH (pdb entry 1v35) was used to investigate the non-competitive inhibition of *Pf*FabI activity. The molecular interaction fields were generated using GRID 22A software (Molecular Discovery) and the energy of binding of ligands to the protein complex was estimated using GLUE module of this software.[29,30] The whole surface of the protein was target for the interaction and all ligands exhibited multiple binding positions on the surface (Fig. 7b), with similar preferences. Importantly, ligands appear to protrude into the protein surface and to make close contacts with the protein substrate. These interactions could possibly affect the protein conformation and therefore inhibiting the protein activity. The 2-HDA protrudes the most of all ligands due to the extended structure around the carboxylic group and possibly has the strongest impact on protein conformation and flexibility.

Molecular properties of HDAs and PA were calculated using ChemSilico and Vega ZZ, which indicated the compliance of 2-HDA with Lipinski's rules.[31] As shown in Table 3, the predicted log *P* values by CS and Vega ZZ of 2-HDA are 5.6 and 5.47, respectively, while the predicted log *P* values of PA are 5.4 and 6.04. The predicted PSA/SA (polar surface areas/surface areas) values and human intestinal absorptions (HIA) of 2-HDA are very similar to those of PA. Since the PA readily crosses the blood–brain barrier (BBB),[32] and the PSA correlates with the ability of molecules to cross the BBB,[33] it is likely that the 2-HDA has a good penetration ability through cell membranes, and will even diffuse through the BBB.

2.6. Inhibitory activity against other parasitic protozoa and primary L6 cells

Finally, the species-specific antiprotozoal activity of the HDAs against *Trypanosoma brucei rhodesiense* (bloodstream forms),

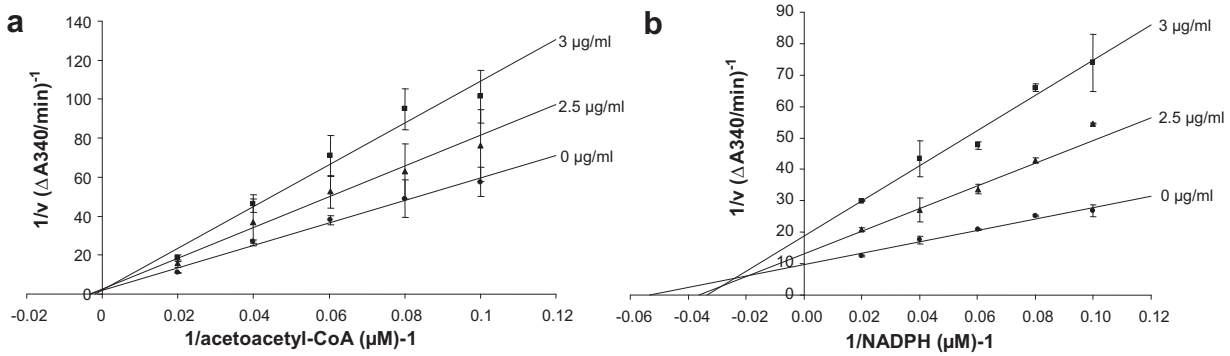

Figure 6. Kinetic plots of the binding of 2-HDA to *Pf*FabG when the substrate acetoacetyl-CoA (a) and the cofactor NADPH (b) was varied.

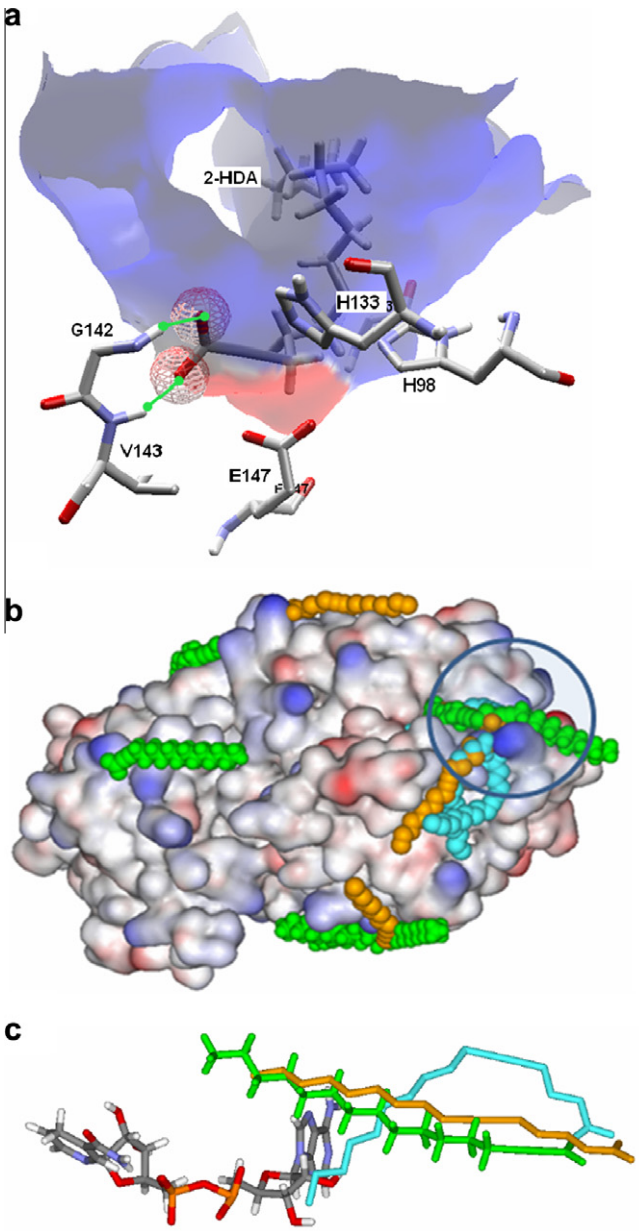

Figure 7. Interaction of acetylenic ligands with *Pf*FabZ and *Pf*FabI predicted by molecular docking: (a) interaction of ligands within the binding site of *Pf*FabZ represented as surface (2-HDA represented as thick sticks inside the surface, green lines depict hydrogen bonds), (b) surface map of electrostatic potentials of the *Pf*FabI with ligands bound to the multiple binding sites (2-HDA—green; 5-HDA—orange; 6-HDA—cyan) and (c) detailed view of the ligands bound to the protein in respect to the substrate at the site encircled in b).

Table 2
Trypanocidal and leishmanicidal activities of the HDAs and PA

Compound	*T. brucei rhodesiense*	*Trypanosoma cruzi*	*Leishmania donovani*	L6 cell cytotoxicity
Standard	0.003[a]	0.489[b]	0.26[c]	0.004[d]
2-HDA	21.1	20.2	4.5	85.9
5-HDA	25.5	>30	13.4	>90
6-HDA	31.7	>30	9.8	30.3
9-HDA	3.7	>30	4.1	80.8
PA	30.4	>30	14.5	52.7

IC_{50} values are in μg/ml and represent the average of at least two independent assays performed in duplicates. Reference compounds [a] melarsoprol; [b] benznidazole; [c] miltefosine; [d] podophyllotoxin.

Table 3
Calculated pharmacokinetic properties of HDAs and PA

Fatty acid	log *P*[a]	log *P*[b]	HIA[a]	PSA[b]	SA[b]	PSA/SA[b] (%)
2-HDA	5.60	5.47	89.1	101.9	599.9	17.0
5-HDA	5.40	5.47	89.1	92.6	635.7	14.6
6-HDA	5.38	5.47	89.1	89.9	640.3	14.0
9-HDA	5.36	5.47	89.1	88.6	632.2	14.0
PA	5.40	6.04	88.8	91.3	615.2	14.8

[a] Calculated by ChemSilico (CS) software.
[b] Calculated by [b]Vega ZZ software log *P*: octanol/water partition coefficient; HIA: Human intestinal absorption; PSA: polar surface area; SA: surface area.

T. cruzi (intracellular amastigotes in L6 rat skeletal myoblasts), and *L. donovani* (axenic amastigotes) was determined. As shown in Table 2, the studied HDAs displayed the best overall antiprotozoal activities against *L. donovani*, with 2-HDA and 9-HDA being equally active (IC_{50}s 4.5 and 4.1 μg/ml). 6-HDA displayed a twofold less activity (IC_{50} 9.8 μg/ml), whereas 5-HDA and PA were the least active ones (IC_{50} 13.4 and 14.5 μg/ml). The 9-HDA displayed the best activity toward *T. b. rhodesiense* with an IC_{50} value of 3.7 μg/ml, while the remaining compounds were 6–10-fold less active. The 2-HDA was the only fatty acid with moderate *T. cruzi* activity (IC_{50} 20.2 μg/ml). Overall, the 9-HDA showed the broadest spectrum antiprotozoal activity. An early study[34] has pointed out the cidal effect of palmitic (hexadecanoic) acid against the promastigote stages of *L. donovani*, *L. tropica* and the epimastigote and trypomastigote stages of *T. cruzi*. To our knowledge, this is the first study assessing trypanocidal and leishmanicidal effects of the four HDAs.

Selective toxicity of all fatty acids was determined against L6 cells, a primary cell line derived from rat skeletal myoblasts. As displayed in Table 2, the 2-HDA shows negligible toxicity and 5-HDA is completely non-toxic at the highest test concentrations (90 μg/ml). Only 6-HDA and PA bear some moderate cytotoxic effects against L6 cells.

3. Discussion

In contrast to easily cultivable BS, working with LS malaria parasites is difficult and costly since primary hepatocytes or hepatoma cells need to be infected with live sporozoites from *Plasmodium*-infected mosquitoes. This requires continuous supply of blood containing infectious gametocytes and a mosquito breeding facility to produce viable, uncontaminated, and infective sporozoites. LS infection has long been unamenable to standard biochemical assays because of generally low infection rates of hepatocytes and hepatoma cells.[35] However, technological developments in the field of microscopy and the generation of parasites with specific cell types expressing fluorescent proteins permitted fascinating live imaging of LS infection. Nowadays, automated microscopy, infrared fluorescence scanning, flow cytometry, and immunofluorescence techniques enable medium to high throughput screening in LS parasites. The current study is the first to investigate the LS malaria parasite growth inhibitory effect of 2-, 5-, 6-, and 9-HDAs, by using rodent *P. yoelii* parasites to infect HepG2:CD81cell line. Infection was assayed by two medium throughput LS growth inhibition assays, FC and IFA. In the FC assay, the HepG2:CD81 cells that are infected with GFP expressing *P. yoelii* sporozoites are exposed to compound for 43 h. The number of GFP-positive hepatoma cells is determined by FC and is used to measure infection rates. One disadvantage of the FC assay is that it only provides information on the LS infection rates after 43 h of post-infection. In order to determine the effects of the drugs on the morphology and development of the LS parasites, we undertook IFAs of

P. yoelii-infected HepG2:CD81 cells after drug treatment. IFA does not only provide data on morphology and the size of LS parasites, but also gives a visual indication of host cytotoxicity. The LS parasites were detected using a mouse monoclonal antibody against *P. berghei* HSP70 that cross-reacts with *P. yoelii* HSP70 and polyclonal antibody against the *P. yoelii* UIS4 protein. While infection rates are difficult to assess from the IFA (because host cell numbers were not counted), the reduction in LS sizes is a more sensitive indicator for the inhibitory effect of a drug on LS development compared to the FC-based assay. As shown in Figures 2 and 3, the 2-HDA was the only acid inhibiting the growth of *P. yoelii* LS parasites in both assays. The IC_{50} values of 2-HDA and the standard, atovaquone, are much smaller in the IFA, showing the sensitivity of the assay.

Most of the current antimalarial agents target the parasite's blood stages. Only a few compounds, such as primaquine, tafenoquine, and atovaquone have activity against the LS parasites, however their use is limited due to hematological toxicity in individuals with G6PD-deficiency and high costs (atovaquone). Although discussed controversially, it is logical and desirable to have one drug with a dual effect on both LS and BS parasites, that is, both prophylactic and therapeutic. Quinine, chloroquine, mefloquine, and artemisinins have little or no efficacy against the hepatic parasites, contributing to the relapse of the disease, particularly in *P. vivax*, which develops liver hypnozoites. An earlier study[20] reported 2-HDA to inhibit the growth of hepatoma cells, however, we observed no toxicity even at the highest test concentrations toward HepG2:CD81 cells by any HDA compounds in any of the assay employed. The HDAs generally lacked toxicity against mammalian L6 cells, indicating a reasonable therapeutic index. Hence, 2-HDA appears to be a promising small molecule for its inhibitory activity on both LS and BS malaria parasites, with good cell viability on hepatic cells. The inhibition of LS by a compound, such as 2-HDA, will also reduce the risk of transmission by interrupting the formation of the gametocytes in late BS. The next logical step would be to test HDAs on *P. vivax* and *P. ovale* hypnozoites. However, none of the rodent *Plasmodium* species including *P. yoelii* produces dormant hepatic stages in laboratory animals[3] hence this could not be performed in our laboratories.

Due to the inherent difficulty in studying the LS parasites, only little progress has been made in the identification of new LS drug targets for rational drug design. Recent studies show the importance of type II FAS in the LS, particularly in the transition point of parasites from liver to blood. As FAS-II deficiency leads to loss of infective capability of red blood cells in vitro and in vivo,[7,8] the plasmodial FAS-II system appears to be a promising drug target for the clinically silent LS infection. So far, only hexachlorophene, a *Pf*FabG inhibitor, was shown to inhibit the LS development in vitro in a dose-dependent manner with an IC_{50} value of 4.8 μM (=1.95 μg/ml).[36] Recently, the potent *Pf*FabI inhibitor triclosan, which was previously reported to inhibit the blood stage *P. falciparum* infection, has been reported to be cidal at the late liver phases of *P. berghei* with an IC_{50} value of 39.4 μM (=11.4 μg/ml).[37] Thus, 2-HDA appears to be the third *Pf*FAS-II inhibitor with activity against LS malaria parasites. The inhibition of multiple *Pf*FAS-II enzymes by 2-HDA is tantalizing, as it bears lower risk to develop resistance. The remaining fatty acids also inhibit *Pf*FabI and *Pf*FabZ moderately and in the FC assay, they cause a 10% decrease in infection (data not shown) at the highest test concentration, 25 μg/ml (data not shown). This might imply that they possibly have some activity at higher concentrations, however, due to toxicity of DMSO against hepatic cells, we were unable to test higher doses. On the other hand, since *Pf*FabZ and *Pf*FabI are inhibited by all compounds, one can suggest that the lack of LS activity of the other HDAs stems from their low penetration into the infected hepatocytes. However, the calculated pharmacokinetic properties of the remaining HDAs were very similar to those of 2-HDA and PA (Table 3), ruling out the permeability as a problem. The good drug-like properties, especially their ability to cross membranes, including the BBB, of HDAs could make them very useful for the treatment of advanced phases of cerebral malaria and sleeping sickness caused by *Trypanosoma brucei rhodesiense*.

It has been reported that 2-HDA competitively inhibits the mycobacterial InhA (*Mt*FabI) enzyme[16] with a similar potency (K_i value 2.1 ± 0.6 μM) to that obtained with *Pf*FabI. Although the exact binding mode of 2-HDA on *Pf*FabI is not completely clear, it is obvious that the significant enzyme inhibitory activity of 2-HDA is not a simple, non-specific detergent effect. Again, similar to its antimycobacterial (and probably antifungal) activity, the hepatic stage parasite activity of 2-HDA does not seem to be due to non-specific fatty acid-mediated lysis. On the other hand, 2-HDA acts as a prodrug and requires metabolization in *Mycobacterium* species.[16] Whether this same phenomenon occurs in *Plasmodium* species remains unclear and warrants further studies.

Our findings concerning LS development were generated with the rodent malaria parasite *P. yoelii*, which has a much shorter LS cycle (50–60 h), but the high conservation of FAS-II among *Plasmodium* species[22] may suggest similar results on *P. falciparum* and *P. vivax* hepatic stage development. In a recent paper, Yu et al. (2008)[8] compared FA profiles of wild-type and FabI-mutant parasites in the blood stage *of P. falciparum* and *P. berghei*. The spectrum of synthesized FA's was different in *P. falciparum* where C-16 and C-18 FAs were detected while in *P. berghei* C-12 to C-24 FAs were predominant.[8] The ^{14}C-acetate (radiolabeled FA precursor) isotope-incorporation studies showed no difference in the FA profiles in the FabI mutant and wild-type blood stages in both *P. falciparum* and *P. berghei* indicating clearly that FAS-II is not involved in the synthesis of these FA species. Thus, the different FAs in the blood stage might be formed by fatty acid elongases and the differences in FA synthesis in the two *Plasmodium* species might be due to the number of involved elongases detected in their genome (three for *P. falciparum*, four for *P. berghei)*.[8] A recent paper by Déchamps et al. (2010)[38] showed that rodent and mammalian *Plasmodium* blood stage parasites differ in their phospholipid pathways. Hence it is possible that lipid metabolic pathways are different in the rodent and human *Plasmodium* and yet the parasite FAS-II pathway will be essentially similar. Since the FAS-II pathway does not appear to be operational in blood stages[7,8] one cannot say that the observed effects by the HDA and/or palmitic acid in the blood and liver stages would be through the same mechanisms.

4. Conclusions

In this study, we report the rapid synthesis and broad antiprotozoal activity of four HDAs. Of the four HDAs studied herein, only the 6-HDA is a natural compound, recently isolated from the plant *Sommera sabiceoides*.[15] Many unsaturated fatty acids, including the natural product scleropyric acid, a C-17 fatty acid with a double and triple bond have been shown to have antiplasmodial activity,[12] but to our knowledge, this is the first report of antimalarial activity of the 2-, 5-, 6-, and 9-HDAs against the BS of *P. falciparum* parasites. The data presented in this manuscript suggest that the presence and the position of the triple bond in the acyl chain to be of paramount importance for determining the antiprotozoal activity of acetylenic C_{16} fatty acids. Considering that the PA was the most active compound against BS *P. falciparum* parasites, it seems that the absence or a more distal position (C-5) of a triple bond is favored for BS activity. However, the presence

of an acetylenic function at C-2 appears to be a critical requirement for LS parasite growth arrest as PA and all other HDAs are inactive. The presence of a triple bond next to the carbonyl group, as found in 2-HDA, seems to increase the conformational flexibility and dipole moment of 2-HDA, thus enabling it to interact with *Pf*FAS-II target enzymes more efficiently. The presence of a single acetylenic function at C-9 however, increases the trypanocidal and leishmanicidal activity of the C_{16} acids significantly. At this point, a relevant question emerges concerning the impact of the chain length, as well the number of triple bonds within the acetylenic acid on their biological activity. We performed a docking study calculating the binding energies of the 2-tetradecynoic acid (2-TDA, C14), the 2-octadecynoic acid (2-ODA, C-18), and the 2,5-hexadecadiynoic acid (2,5-HDDA). This study showed that 2-HDA was still the best binder toward the two target *Pf*FAS-II enzymes, *Pf*FabG and *Pf*FabZ (data not shown). The strength or mode of binding of 2-TDA and the 2-ODA against *Pf*FabI was different, which may indicate a weaker or the absence of activity. The 2,5-HDDA had close binding energies to 2-HDA toward *Pf*FabG and *Pf*FabZ, but better binding energy toward *Pf*FabI. However, the orientation of the 2,5-HDDA molecule in the binding region is different due to steric constraints of triple bond combination, thus it might not have the same inhibitory activity as the 2-HDA. These calculations confirm that the C-16 HDAs were a good choice for this study and 2-HDA had better activity against a wider range of target enzymes. The in vitro activity of 2-TDA, 2-ODA, and 2,5-HDDA, however, needs to be assessed in whole cell parasite assays, following their successful synthesis.

In conclusion, the current study has identified acetylenic C_{16} acids as a novel class of antiprotozoal agents. The discovery of these easily synthesizable fatty acids with promising antimalarial and malaria prophylactic effects may represent an opportunity for the development of new agents, particularly those derived from 2-HDA, for the control and potentially eradication of malaria. Taking into account their synthetic accessibilities, antiprotozoal potencies, no apparent toxicity on hepatocytes at active concentrations, ability to affect both BS and LS malaria parasites, as well as good pharmaceutical (lipophilic) and pharmacokinetic properties, the acetylenic acids, in particular 2-HDA, might be useful tools to understand the potential of fatty acids as drug candidates. Our future work will involve the synthesis, in vitro and in vivo evaluation of more potent acetylenic fatty acids with multiple triple and double bonds.

5. Experimental

5.1. General

(Trimethylsilyl)-acetylene and other reagents used were purchased from Aldrich, TCI America, and Alfa Aesar. All synthetic products were analyzed by ^1H and ^{13}C Nuclear Magnetic Resonance (NMR) using a Bruker Avance DRX-500 or a Bruker Avance DPX-300. The samples were dissolved in chloroform-*d* ($CDCl_3$) and the solvent signals at 7.26 and 77.0 ppm were used as internal standard for proton and carbon, respectively. Mass spectral data were acquired on a GC–MS (Hewlett–Packard 5972A MS Chem Station) instrument at 70 eV, equipped with a 30 m × 0.25 mm special performance capillary column (HP-5MS) of polymethylsiloxane cross-linked with 5% phenyl methylpolysiloxane. The GC–MS analysis conditions were identical to those previously described.[39] Infrared (IR) spectra were recorded on a Nicolet 600 FTIR spectrophotometer. Melting points (°C, uncorrected) were determined in a MEL-TEMP capillary melting point apparatus. Thin layer chromatography was carried out on aluminium TLC plates pre-coated with Silica Gel 60 F254 (Merck, 0.25 mm).

5.2. Synthesis and structure elucidation of the 5-, 6-, and 9-HDAs

5.2.1. Alkyne couplings with the bromoalkyloxy-*tert*-butyldimethylsilanes

To a stirred solution of the alkyne (3.74–4.36 mmol), prepared from the bromoalcohol and *tert*-butyldimethylsilylchloride, in dry THF (5.0–15.0 ml), *n*-Buli (2.5 M, 10.90–11.22 mmol) in dry hexane was added dropwise while keeping the temperature at −60 °C. After 45 min, HMPA (1.12–10.0 ml) and the bromoalkyloxy-*tert*-butyldimethylsilane (3.74–4.36 mmol) were added dropwise to the reaction mixture at −60 °C. After 24 h, the reaction mixture was worked up by pouring into a large volume of water and extracting with diethyl ether (2 × 15 ml). The organic layer was washed with brine (1 × 15 ml) before drying ($MgSO_4$). Filtration, rotoevaporation of the solvent, and fractional distillation afforded the *tert*-butyldimethylsilyloxy-alkynes in 23–32% yields after purification by Kugelrohr distillation (130–137 °C/3 mmHg) of the impurities.

5.2.2. Oxidation to the carboxylic acids

To a stirred solution of the alkynol (0.2–1.3 mmol), after deprotection with *tert*-butylammonium fluoride (TBAF), in 3.0–7.0 ml of DMF was slowly added pyridinium dichromate (0.8–7.9 mmol) at rt. After 24–48 h, the reaction mixture was worked up by pouring 10 ml of water and extracting with hexane (3 × 12 ml). Once the solvent was evaporated and dried in vacuo, the acetylenic fatty acids were obtained in 40–70% yields.

5.2.2.1. 5-Hexadecynoic acid (5-HDA). 5-HDA was obtained in a 75% yield (249 mg) from the reaction of 313 mg (1.3 mmol) of 5-hexadecyn-1-ol with 3.0 g (7.9 mmol) of pyridinium dichromate. IR (neat) ν_{max} 3105–2900, 2926, 2854, 2206, 1711, 1465, 1261, 1207, 1090, 920, 803, 722 cm^{-1}. ^1H NMR (500 MHz, $CDCl_3$) δ_H 2.48 (2H, t, J = 7.5 Hz, H-2), 2.12 (4H, m, H-4, H-7), 1.80 (2H, quintet, J = 7.2 Hz, H-3), 1.46 (2H, quintet, J = 7.3 Hz, H-8), 1.35–1.25 (14H, m, $-CH_2-$), 0.88 (3H, t, J = 6.9 Hz, H-16). ^{13}C NMR (125 MHz, $CDCl_3$) δ_C 178.5 (s, C-1), 81.5 (s), 78.5 (s), 32.6 (t, C-2), 31.9 (t, C-14), 29.6 (t), 29.5 (t), 29.3 (t), 29.1 (t), 29.0 (t), 28.9 (t), 24.0 (t), 22.7 (t), 18.7 (t, C-7), 18.3 (t, C-4), 14.1 (q, C-16).

5.2.2.2. 6-Hexadecynoic acid (6-HDA). 6-HDA was obtained in a 42% yield (87 mg) from the reaction of 195 mg (0.8 mmol) of 6-hexadecyn-1-ol with 1.2 g (3.3 mmol) of pyridinium dichromate. IR (neat) ν_{max} 3105–2900, 2927, 2851, 1709, 1469, 1260, 1207, 1077, 899, 797, 718 cm^{-1}. ^1H NMR (300 MHz, $CDCl_3$) δ_H 2.37 (2H, t, J = 7.4 Hz, H-2), 2.15 (4H, m, H-5, H-8), 1.78–1.26 (19H, m, $-CH_2-$), 0.87 (3H, t, J = 6.7 Hz, H-16). ^{13}C NMR (75 MHz, $CDCl_3$) δ_C 179.9 (s, C-1), 80.8 (s), 79.3 (s), 33.4 (t, C-2), 31.9 (t), 29.5 (t), 29.3 (t), 29.15 (t), 29.10 (t), 28.9 (t), 28.4 (t), 23.8 (t), 22.7 (t), 18.7 (t), 18.4 (t), 14.1 (q, C-16).

5.2.2.3. 9-Hexadecynoic acid (9-HDA). 9-HDA was obtained in an 80% yield (60 mg) from the reaction of 70 mg (0.25 mmol) of 9-hexadecynal with a $NaClO_2$–NaH_2PO_4 buffer solution. IR (neat) ν_{max} 3313–2900, 2954, 2929, 2852, 1690, 1465, 1441, 1414, 1335, 1277, 1263, 1094, 1015, 918, 726 cm^{-1}. ^1H NMR (300 MHz, $CDCl_3$) δ_H 2.34 (2H, t, J = 7.5 Hz, H-2), 2.13 (4H, m, H-8, H-11), 1.63 (2H, quintet, J = 7.0 Hz, H-3), 1.46 (4H, quintet, J = 6.4 Hz, H-7, H-12), 1.30 (12 H, m, $-CH_2-$), 0.87 (3H, t, J = 6.5 Hz, H-16). ^{13}C NMR (75 MHz, $CDCl_3$) δ_C 179.9 (s, C-1), 80.4 (s), 80.0 (s), 34.0 (t, C-2), 31.5 (t), 29.7 (t), 29.1 (t), 29.0 (t), 28.9 (t), 28.8 (t), 28.6 (t), 28.5 (t), 24.6 (t), 22.6 (t), 18.75 (t), 18.71 (t), 14.1 (q, C-16).

5.3. 2-Hexadecynoic acid (2-HDA)

2-HDA was obtained as a white solid in a 10% yield from the reaction of 1-pentadecyne (1.00 g, 4.8 mmol) and excess dry CO_2. Mp 49–51 °C. IR (neat) ν_{max} 3400–2900 (br), 2914, 2848, 2235, 1679, 1467, 1409, 1277, 1077 cm^{-1}. ^1H NMR (500 MHz, $CDCl_3$) δ_H 2.35 (2H, t, J = 7.2 Hz, H-4), 1.59 (2H, quintet, J = 7.4 Hz, H-5), 1.41–1.22 (20H, m, $-CH_2-$), 0.88 (3H, t, J = 7.0 Hz, H-16). ^{13}C NMR (125 MHz, $CDCl_3$) δ_C 157.2 (s, C-1), 92.6 (s, C-3), 72.5 (s, C-2), 31.9 (t, C-14), 29.65 (t), 29.63 (t), 29.6 (t), 29.4 (t), 29.3 (t), 29.0 (t), 28.8 (t), 27.4 (t), 22.7 (t, C-15), 18.8 (t, C-14), 14.1 (q, C-16).

5.4. Antimalarial activity against blood stage (BS) *P. falciparum*

In vitro activity against erythrocytic stages of *P. falciparum* was determined by a modified [^{3}H]-hypoxanthine incorporation assay,[40] using the chloroquine- and pyrimethamine-resistant K1 strain and the standard drug chloroquine. Briefly, parasite cultures incubated in RPMI 1640 medium with 5% Albumax (without hypoxanthine) were exposed to serial drug dilutions in microtiter plates. After 48 h of incubation at 37 °C in a reduced oxygen atmosphere, 0.5 μCi ^{3}H-hypoxanthine was added to each well. Cultures were incubated for a further 24 h before they were harvested onto glass-fiber filters and washed with distilled water. The radioactivity was counted using a Betaplate™ liquid scintillation counter (Wallac, Zurich, Switzerland). The results were recorded as counts per minute (CPM) per well at each drug concentration and expressed as percentage of the untreated controls. IC_{50} values were calculated from graphically plotted dose–response curves.

5.5. Antimalarial activity against liver stage (LS) *P. yoelii*

To assay for inhibitory activity against *Plasmodium* liver stages, two assays based on in vitro infections of *P. yoelii* in the hepatoma cell line HepG2:CD81 were developed. HepG2:CD81 cells stably express the CD81 protein that is necessary and sufficient to give high infection rates with *P. yoelii* sporozoites in vitro.[41] *P. yoelii* wild-type and transgenic *P. yoelii* sporozoites that express green fluorescent protein (PyGFP)[42] parasites were cycled between *Anopheles stephensi* mosquitoes and swiss-webster mice (Harlan). Infected mosquitoes were maintained at 24 °C and 70% humidity on sugar water (dextrose). The first assay is a flow cytometry-based analysis using the BD-LSRII (BD Biosciences) flow cytometer. Briefly, 100,000 HepG2:CD81 cells grown in complete media (advanced DMEM/F12 supplemented with 10 FBS, 2% penicillin/streptomycin, 2% glutamine and 1% amphotericin) were seeded in 48 well plates previously coated with 20 μg/ml ECL attachment matrix (Upstate Labs). The day after the cells were seeded, they were infected with 50,000 PyGFP sporozoites (in RPMI media at a volume of 100 μl/well) that were isolated from manually dissected PyGFP-infected mosquitoes 14 days post-blood meal. Two hours after the sporozoites were added, media in each well were removed and replaced with fresh complete media containing various concentrations of compounds. The HepG2:CD81 infected cells were continuously exposed to the compounds with a media change 24 h after infection and allowed to develop for a further 43 h at 37 °C in a CO_2 incubator. The cells were trypsinized to prepare a single cell suspension, centrifuged, and resuspended in 100 μl complete medium containing 0.1% 7-amino-actinomycin D (7-AAD, Invitrogen), an impermeant nucleic acid dye that could be used to stain membrane-compromised cells (i.e., dead cells). After transfer to 96-well v-bottom plates, the number of GFP-positive hepatoma cells is determined by flow cytometry using the BD-LSRII HTS system. In most cases the BD-LSRII can count 50,000–100,000 events from each well with 1.5–2.0% GFP-positive cells in wells treated with 0.5% or 1.0% DMSO (untreated control). Compounds were prepared as 10 mM solutions in DMSO and tested at concentrations of 10–100 μM in complete media. Atovaquone, a drug with known LS inhibitory activity,[25] was used as a positive control.

To verify the results of the FC assay and to determine the effect of the compounds on the morphology and development of the LS parasites, immunofluorescence analysis (IFAs) of *P. yoelii*-infected HepG2:CD81 cells after compound treatment was also carried out. Subconfluent HepG2:CD81 cells that were seeded in 8-well chambered slides (Nunc) and maintained at 37 °C in 5% CO_2 and subsequently treated with the compounds. After 43 h of incubation, the infected cells were fixed with 10% neutral buffered formalin. IFA was carried out using a mouse monoclonal antibody against the *Plasmodium* HSP70 protein together with a rabbit polyclonal antibody raised against either the *P. yoelii* UIS4 or FabI proteins. The second antibody was used to confirm the presence of the liver stage parasite. The slides were scanned with a fluorescence microscope and images were captured using a 20× objective. The resulting images were analyzed with the METAMORPH program (Molecular Devices) which allows for automated measurements of liver stage parasites stained with the HSP70 antibody (Fig. 2). Approximately 20–25 liver stage parasites were measured for each compound treatment and the average sizes were compared with DMSO-treated controls. The normalized reduction in liver stages from infections treated with the compounds compared with DMSO-treated controls was calculated and used for IC_{50} estimation using the ICESTIMATOR program (http://bichat.inserm.fr/equipes/Emi0357/Palu/index.htm). Compounds were dissolved in DMSO and tested at concentrations up to 25 μg/ml in complete media. Atovaquone was used as a positive control. An 100× oil immersion objective was used for the close-up images (Fig. 3).

5.6. Toxicity assessments toward HepG2:CD81 cells

Toxicity of the compounds to HepG2:CD81 cells was determined by using the non-membrane permeant nuclear stain 7-aminoactinomycin D (7-AAD). This stain is generally excluded from live cells and thus generally stains only dead cells. The proportion of 7-AAD positive cells detected in the flow assay is used an indicator for dead cells in the HepG2:CD81 cell culture and thus when compared to %7-AAD-positive cells in DMSO-treated cells can be used as an indirect measure for toxicity of the compounds in the treated cultures. In the IFA, toxicity of the compounds was assessed by comparing the DAPI staining of infected HepG2:CD81 cells treated with DMSO alone or with various concentrations of the compounds. Toxic concentrations of drugs such as high concentrations of atovaquone result in cell death and detachment from the culture slides which result in less DAPI-stained cells.

5.7. Plasmodial FAS-II enzyme inhibition assays and enzyme kinetics

Expression and purification of the *Pf*Fab enzymes as well as the assays were performed as described.[26] Briefly, assays were monitored using an Uvikon 941 Plus spectrophotometer (Kontron Instruments) in 1.0 ml of 20 mM HEPES pH 7.4, and 150 mM NaCl. Compounds were dissolved in DMSO (max. final concentration is 1%). For *Pf*FabI 100 μM NADH (cofactor, Sigma) was added to 1 μg enzyme and the reaction was started by addition of 50 μM crotonyl-CoA (substrate, Sigma). The change of absorbance of the mixture was recorded spectrophotometrically at 340 nm during 1 min. Triclosan was used as a positive control and was analyzed the same way. For *Pf*FabG different cofactor (NADPH, Fluka) and substrate (acetoacetyl-CoA, Sigma) were used. *Pf*FabZ was measured at 263 nm for 2 min in the presence of 25 μM crotonoyl-CoA and 0.5 μg enzyme. Reference compound for the latter

two enzymes was (−)-epigallocatechin gallate (Sigma). IC_{50} values were estimated from graphically plotted dose–response curves.[26]

The inhibition mechanism for 2-HDA was determined under Michaelis–Menten steady-state conditions. For *Pf*FabI, with respect to the substrate, 1 μg enzyme was incubated with a fixed NADH concentration (100 μM) and increasing inhibitor concentrations (0–1 μg/ml). The reaction was initiated by the addition of crotonyl-CoA (10–50 μM). The inhibition mechanism with respect to NADH was determined in a similar way. For this, *Pf*FabI was incubated with varying NADH concentrations (10–50 μM) and different inhibitor concentrations (0–1 μg/ml). The reaction was initiated by the addition of 50 μM crotonyl-CoA. Kinetic studies for *Pf*FabG were performed in a similar way, using NADPH as cofactor and acetoacetyl-CoA as substrate. For *Pf*FabZ, 0.5 μg enzyme was incubated with increasing inhibitor concentrations (0–1 μg/ml) and the reaction was started by the addition of crotonyl-CoA (10–50 μM). K_i values were obtained from Dixon and secondary plots. The reported values represent means of two independent experiments.

5.8. Molecular modeling and pharmacokinetic calculations

The 3D structure of ligands used for the docking were built by Maestro GUI v8.5 (Schrodinger LLC) and initial conformations with the correct protonation states were generated using LigPrep (Schrodinger LLC) and OPLS-2005 force field. The protein structures FabZ (id:1z6b), FabI (id:1v35), and FabG (id:2c07) were downloaded from the RCSB Protein Data Bank (PDB) and prepared for docking by Rebol script 'Receptor.r' implemented in VegaZZ.[43] The calculations of ligands docking to the binding site of *Pf*FabZ and *Pf*FabG were carried out using Autodock and Gridock and VegaZZ as graphic user interface. Binding site was centered on the residues of the active site a cube with an edge length of 32 Å was defined as a bounding box in the protein. The best pose generated for each ligand was selected based on lowest energy value of the Autodock scoring function. The docking calculations of ligands into the *Pf*FabI were carried out using GLUE program (GRID package from MolDiscovery Ltd). The surface of the whole protein was selected to generate GRID maps for the probes that best simulate ligands. The docking was carried out taking into account electrostatic contributions and flexibility of ligands at default values of GLUE settings. Interaction energies scores (kcal/mol) were used to rank the interaction between ligand and a protein, but all solutions were considered in the analysis of the results. The pharmacokinetics and estimated molecular properties of ligands were estimated using Vega ZZ software and ChemSilico online server (http://www.chemsilico.com).

5.9. Trypanocidal activity against *Trypanosoma brucei rhodesiense*

STIB 900 strain of *T. b. rhodesiense* and the standard drug melarsoprol were used for the assay. This stock was isolated in 1982 from a human patient in Tanzania and after several mouse passages cloned and adapted to axenic culture conditions.[44] Minimum Essential Medium (50 μl) supplemented with 25 mM HEPES, 1 g/l additional glucose, 1% MEM non-essential amino acids (100×), 0.2 mM 2-mercaptoethanol, 1 mM Na-pyruvate, and 15% heat inactivated horse serum was added to each well of a 96-well microtiter plate.[45] Serial drug dilutions of seven threefold dilution steps covering a range from 90 to 0.123 μg/ml were prepared. Then 10^4 bloodstream forms of *T. b. rhodesiense* STIB 900 in 50 μl was added to each well and the plate incubated at 37 °C under a 5% CO_2 atmosphere for 72 h. 10 μl of a resazurin solution (12.5 mg resazurin dissolved in 100 ml double-distilled water) was then added to each well and incubation continued for a further 2–4 h. Then the plates were read in a Spectramax Gemini XS microplate fluorometer (Molecular Devices Cooperation, Sunnyvale, CA, USA) using an excitation wavelength of 536 nm and an emission wavelength of 588 nm. Data were analyzed using the microplate reader software Softmax Pro (Molecular Devices Cooperation, CA, USA).

5.10. Trypanocidal activity against *T. cruzi*

Rat skeletal myoblasts (L6 cells) were seeded in 96-well microtitre plates at 2000 cells/well in 100 μL RPMI 1640 medium with 10% FBS and 2 mM l-glutamine. After 24 h the medium was removed and replaced by 100 μl per well containing 5000 trypomastigote forms of *T. cruzi* Tulahuen strain C2C4 containing the β-galactosidase (Lac Z) gene.[46] After 48 h, the medium was removed from the wells and replaced by 100 μl fresh medium with or without a serial drug dilution of seven threefold dilution steps covering a range from 90 to 0.123 μg/ml. After 96 h of incubation the plates were inspected under an inverted microscope to assure growth of the controls and sterility. Then the substrate CPRG/Nonidet (50 μl) was added to all wells. A color reaction developed within 2–6 h and could be read photometrically at 540 nm. Data were transferred into the graphic programme Softmax Pro (Molecular Devices), which calculated IC_{50} values. Benznidazole was the standard drug used.

5.11. Leishmanicidal activity against *L. donovani*

Amastigotes of *L. donovani* strain MHOM/ET/67/L82 were grown in axenic culture at 37 °C in SM medium at pH 5.4 supplemented with 10% heat-inactivated fetal bovine serum under an atmosphere of 5% CO_2 in air. One hundred microliters of culture medium with 10^5 amastigotes from axenic culture with or without a serial drug dilution were seeded in 96-well microtitre plates. Serial drug dilutions covering a range from 90 to 0.123 μg/ml were prepared. After 72 h of incubation the plates were inspected under an inverted microscope to assure growth of the controls and sterile conditions. Ten microliters of a resazurin solution (12.5 mg resazurin dissolved in 100 ml double-distilled water)[47] was then added to each well and the plates were incubated for another 2 h. Then the plates were read in a Spectramax Gemini XS microplate fluorometer using an excitation wavelength of 536 nm and an emission wavelength of 588 nm. Data were analyzed using the software Softmax Pro. Decrease of fluorescence (=inhibition) was expressed as percentage of the fluorescence of control cultures and plotted against the drug concentrations. From the sigmoidal inhibition curves the IC_{50} values were calculated. Miltefosine was used as a reference drug.

5.12. Cytotoxicity against L6 cells

Assays were performed in 96-well microtiter plates, each well containing 100 μl of RPMI 1640 medium supplemented with 1% L-glutamine (200 mM) and 10% fetal bovine serum, and 4×10^4 L6 cells (a primary cell line derived from rat skeletal myoblasts). Serial drug dilutions of seven threefold dilution steps covering a range from 90 to 0.123 μg/ml were prepared. After 72 h of incubation the plates were inspected under an inverted microscope to assure growth of the controls and sterile conditions. 10 μl of a resazurin solution (12.5 mg resazurin dissolved in 100 ml distilled water) was then added to each well and the plates were incubated for another 2 h. Then the plates were read with a Spectramax Gemini XS microplate fluorometer using an excitation wavelength of 536 nm and an emission wavelength of 588 nm. Data were analysed using the microplate reader software Softmax Pro. Podophyllotoxin was the standard drug used.

Acknowledgments

Part of the project described herein was supported by Award Number SC1GM084708 from the National Institute of General Medical Sciences (N.M.C) and partly by grants from the Bill and Melinda Gates Foundation and Medicines for Malaria Ventures (S.H.K.). The content is solely the responsibility of the authors and does not necessarily represent the official views of the National Institute of General Medical Sciences or the National Institutes of Health. Ina L. Lauinger thanks the School of Pharmacy for the PhD scholarship.

References and notes

1. World Health Organization. World malaria report 2008, Geneva, Switzerland, 2008. http://malaria.who.int/wmr2008/malaria2008.pdf.
2. Greenwood, B. M.; Fidock, D. A.; Kyle, D. E.; Kappe, S. H. I.; Alonso, P. L.; Collins, F. H.; Duffy, P. E. *J. Clin. Invest.* **2008**, *118*, 1266.
3. Mazier, D.; Rénia, L.; Snounou, G. *Nat. Rev. Drug Disc.* **2009**, *8*, 854.
4. Wells, T. N.; Burrows, J. N.; Baird, J. K. *Trends Parasitol.* **2010**, *26*, 145.
5. Carraz, M.; Jossang, A.; Franetich, J. F.; Siau, A.; Ciceron, L.; Hannoun, L.; Sauerwein, R.; Frappier, F.; Rasoanaivo, P.; Snounou, G.; Mazier, D. *PLoS Med.* **2006**, *3*, e513.
6. Mahmoudi, N.; Garcia-Domenech, R.; Galvez, J.; Farhati, K.; Franetich, J. F.; Sauerwein, R.; Hannoun, L.; Derouin, F.; Danis, M.; Mazier, D. *Antimicrob. Agents Chemother.* **2008**, *52*, 1215.
7. Vaughan, A. M.; O'Neill, M. T.; Tarun, A. S.; Camargo, N.; Phuong, T. M.; Aly, A. S.; Cowman, A. F.; Kappe, S. H. *Cell. Microbiol.* **2009**, *11*, 506.
8. Yu, M.; Kumar, T. R.; Nkrumah, L. J.; Coppi, A.; Retzlaff, S.; Li, C. D.; Kelly, B. J.; Moura, P. A.; Lakshmanan, V.; Freundlich, J. S.; Valderramos, J. C.; Vilcheze, C.; Siedner, M.; Tsai, J. H.; Falkard, B.; Sidhu, A. B.; Purcell, L. A.; Gratraud, P.; Kremer, L.; Waters, A. P.; Schiehser, G.; Jacobus, D. P.; Janse, C. J.; Ager, A.; Jacobs, W. R., Jr.; Sacchettini, J. C.; Heussler, V.; Sinnis, P.; Fidock, D. A. *Cell Host Microbe* **2008**, *4*, 567.
9. Surolia, N.; Surolia, A. *Nat. Med.* **2001**, *7*, 167.
10. Krugliak, M.; Deharo, E.; Shalmiev, G.; Sauvain, M.; Moretti, C.; Ginsburg, H. *Exp. Parasitol.* **1995**, *81*, 97.
11. Kumaratilake, L. M.; Robinson, B. S.; Ferrante, A.; Poulos, A. *J. Clin. Invest.* **1992**, *89*, 961.
12. Suksamrarn, A.; Buaprom, M.; Udtip, S.; Nuntawong, N.; Haritakun, R.; Kanokmedhakul, S. *Chem. Pharm. Bull.* **2005**, *53*, 1327.
13. Suksamrarn, A.; Shanks, L. *Can. J. Microbiol.* **1978**, *24*, 593.
14. Konthikamee, W.; Gilbertson, J. R.; Langkamp, H.; Gershon, H. *Antimicrob. Agents Chemother.* **1982**, *22*, 805.
15. Li, X. C.; Jacob, M. R.; Khan, S. I.; Ashfaq, M. K.; Babu, K. S.; Agarwal, A. K.; ElSohly, H. N.; Manly, S. P.; Clark, A. M. *Antimicrob. Agents Chemother.* **2008**, *52*, 2442.
16. Morbidoni, H. R.; Vilcheze, C.; Kremer, L.; Bittman, R.; Sacchettini, J. C.; Jacobs, W. R., Jr. *Chem. Biol.* **2006**, *13*, 297.
17. Wood, R.; Lee, T.; Gershon, H. *Lipids* **1980**, *15*, 141.
18. Wood, R.; Lee, T. *J. Biol. Chem.* **1981**, *256*, 12379.
19. Tasdemir, D.; Topaloglu, B.; Perozzo, R.; Brun, R.; O'Neill, R.; Carballeira, N. M.; Zhang, X.; Tonge, P. J.; Linden, A.; Rüedi, P. *Bioorg. Med. Chem.* **2007**, *15*, 6834.
20. Upreti, G. C.; Matocha, M.; Wood, R. *Lipids* **1981**, *16*, 315.
21. Ames, D. E.; Covell, A. N. *J. Chem. Soc.* **1963**, 775.
22. Carlton, J. M.; Angiuoli, S. V.; Suh, B. B.; Kooij, T. W.; Pertea, M.; Silva, J. C.; Ermolaeva, M. D.; Allen, J. E.; Selengut, J. D.; Koo, H. L.; Peterson, J. D.; Pop, M.; Kosack, D. S.; Shumway, M. F.; Bidwell, S. L.; Shallom, S. J.; van Aken, S. E.; Riedmuller, S. B.; Feldblyum, T. V.; Cho, J. K.; Quackenbush, J.; Sedegah, M.; Shoaibi, A.; Cummings, L. M.; Florens, L.; Yates, J. R.; Raine, J. D.; Sinden, R. E.; Harris, M. A.; Cunningham, D. A.; Preiser, P. R.; Bergman, L. W.; Vaidya, A. B.; van Lin, L. H.; Janse, C. J.; Waters, A. P.; Smith, H. O.; White, O. R.; Salzberg, S. L.; Venter, J. C.; Fraser, C. M.; Hoffman, S. L.; Gardner, M. J.; Carucci, D. J. *Nature* **2002**, *419*, 512.
23. Tsuji, M.; Mattei, D.; Nussenzweig, R. S.; Eichinger, D.; Zavala, F. *Parasitol. Res.* **1994**, *80*, 16.
24. Mueller, A. K.; Camargo, N.; Kaiser, K.; Andorfer, C.; Frevert, U.; Matuschewski, K.; Kappe, S. H. *Proc. Natl. Acad. Sci. U.S.A.* **2005**, *102*, 3022.
25. Davies, C. S.; Pudney, M.; Nicholas, J. C.; Sinden, R. E. *Parasitology* **1993**, *106*, 1.
26. Tasdemir, D.; Lack, G.; Brun, R.; Rüedi, P.; Scapozza, L.; Perozzo, R. *J. Med. Chem.* **2006**, *49*, 3345.
27. Kimber, M. S.; Martin, F.; Lu, Y.; Houston, S.; Vedadi, M.; Dharamsi, A.; Fiebig, K. M.; Schmid, M.; Rock, C. O. *J. Biol. Chem.* **2004**, *279*, 52593.
28. Swarnamukhi, P. L.; Sharma, S. K.; Bajaj, P.; Surolia, N.; Surolia, A.; Suguna, K. *FEBS Lett.* **2006**, *580*, 2653.
29. Goodford, P. J. *J. Med. Chem.* **1985**, *28*, 849.
30. Pidugu, L. S.; Kapoor, M.; Surolia, N.; Surolia, A.; Suguna, K. *J. Mol. Biol.* **2004**, *343*, 147.
31. Lipinski, C. A.; Lombardo, F.; Dominy, B. W.; Feeney, P. J. *Adv. Drug Delivery Rev.* **1997**, *23*, 3.
32. Ouellet, M.; Emond, V.; Chen, C. T.; Julien, C.; Bourasset, F.; Oddo, S.; LaFerla, F.; Bazinet, R. P.; Calon, F. *Neurochem. Int.* **2009**, *55*, 476.
33. Fu, X. C.; Song, Z. F.; Fu, C. Y.; Liang, W. Q. *Pharmazie* **2005**, *60*, 354.
34. Cunningham, L. V.; Kazan, B. H.; Kuwahara, S. S. *J. Gen. Microbiol.* **1972**, *70*, 491.
35. Rankin, K. E.; Graewe, S.; Heussler, V. T.; Stanway, R. R. *Cell. Microbiol.* **2010**, *12*, 569.
36. Tarun, A. S.; Peng, X.; Dumpit, R. F.; Ogata, Y.; Silva-Rivera, H.; Camargo, N.; Daly, T. M.; Bergman, L. W.; Kappe, S. H. *Proc. Natl. Acad. Sci. U.S.A.* **2008**, *8*, 305.
37. Singh, A. P.; Surolia, N.; Surolia, A. *IUBMB Life* **2009**, *61*, 923.
38. Déchamps, S.; Maynadier, M.; Wein, S.; Gannoun-Zaki, L.; Maréchal, E.; Vial, H. J. *J. Lipid Res.* **2010**, *51*, 81.
39. Carballeira, N. M.; Cartagena, M. M.; Fernández Prada, C.; Fernández Rubio, C.; Balaña-Fouce, R. *Lipids* **2009**, *44*, 953.
40. Matile, H.; Pink, J. R. L. In *Immunological Methods*; Lefkovits, I., Pernis, B., Eds.; Academic Press: San Diego, 1990; pp 221–234.
41. Silvie, O.; Rubinstein, E.; Franetich, J. F.; Prenant, M.; Belnoue, E.; Renia, L.; Hannoun, L.; Eling, W.; Levy, S.; Boucheix, C.; Mazier, D. *Nat. Med.* **2003**, *9*, 93.
42. Tarun, A. S.; Baer, K.; Dumpit, R. F.; Gray, S.; Lejarcegui, N.; Frevert, U.; Kappe, S. H. *Int. J. Parasitol.* **2006**, *36*, 1283.
43. Pedretti, A.; Villa, L.; Vistoli, G. *J.C.A.M.D.* **2004**, *18*, 167.
44. Baltz, T.; Baltz, D.; Giroud, C.; Crockett, J. *EMBO J.* **1985**, *4*, 1273.
45. Thuita, J. K.; Karanja, S. M.; Wenzler, T.; Mdachi, R. E.; Ngotho, J. M.; Kagira, J. M.; Tidwell, R.; Brun, R. *Acta Trop.* **2008**, *108*, 6.
46. Buckner, F. S.; Verlinde, C. L.; La Flamme, A. C.; Van Voorhis, W. C. *Antimicrob. Agents Chemother.* **1996**, *40*, 2592.
47. Mikus, J.; Steverding, D. *Parasitol. Int.* **2000**, *48*, 265.